Theoretical Study of Reactive Powder Concrete Deep Beams

Ragheed Fatehi Makki

Civil Engineering Department, University of kufa, kufa, Iraq

Ragheed.Almutwali@uokufa.edu.iq

Ali Talib Jassem

Civil Engineering Department, University of kufa, kufa, Iraq

alit.albozwaida@uokufa.edu.iq

Aseel Sultan Ridha

Civil Engineering Department, University of kufa, kufa, Iraq

aseel.aseel.1979@gmail.com

Abstract

In the present work, the nonlinear finite element method (FEM) analysis by using package ANSYS V.11 has been carried out to analyze eleven tested RPC deep beams, have dimensions 150mm width, 400 mm depth and 1250 mm total length. The present research objective is to analyze the tested RPC deep beams by using three-dimensional nonlinear finite element (ANSYS Version 11.0) computer program was used in this work. Eight-node brick elements (SOLID 65) are used to represent the concrete and three dimensional (LINK 180) is a spar (or truss) element are used to represent the steel reinforcement and element (SOLID 185) is used for the steel plates modeling. This compare between the numerical and experimental conclusion assured well airworthiness from this numerical analysis and this methodology developable in this study where this maximal distinction rate in this ultimate loading was about below 4.2% to total this tested and analyzed RPC deep beams.

Keywords: - Theoretical Study, 3DFinite Element, Reactive Powder concrete, Deep beams.

1. Introduction

Reactive Powder Concrete is the ultra-high strength and great ductilities combined material by advancer mechanically characteristics. Reactive Powder Concrete is the steel fibers (Vf), superplasticized, silica fume (SF), cement mixture by well little water-cement rate (w/c) properties with a presence from very fine quartz sand (0.15-0.60 mm) alternatively normal aggregate [1].

According to the ACI code Provisions for shear , deep beams are members with length of clear span measured face to face of supports(ℓn) not exceeding four times total depth (h) (ℓn ≤ 4h) or region of beams with concentrated loads within a distance (a) two times the total depth measured from the support (a ≤ 2h) that is loaded on one face and supported on the opposite face [2].

This enhanced for reminder this numerical studied was an approximative in this excrete prioritizes much factors mostly[3]: (1) An approximation in this material modeling from concrete and steel (2) An approximation immanent in this finite element technique (3)An approximation in this integration function use in this numerical analysis(4)Approximation submitted due to this type from procedure use for solve this nonlinear system from equations.

In the present work, a finite element analysis done by ANSYS V.11 for eleven tested specimens. Comparison of the Load - Deflection curves of the finite element analysis and the experimental tests are discussed ,furthermore three study cases are discussed .

In 2012, Kadri, et al. [4] investigated the compressive strength of the silica fume concretes at below (w/c) materials rate by the naphthalene sulphonate super plasticizer. It was found the raise the compressive strength of silica fume concretes depends very major on the reduction of the (w/c) materials rate that on the surrogate of the (SF) by cement. It was also shown that the compressive strength raise by the (SF) contented up to the (20%) and scopes a maximum amount for the (10%) to (15%) silica fume matched.

In 2013, Bashandy et al. [5] calculated the effects of exalted heat of the (200, 300and 500) ℃ as two and four hours on the major mechanical- characteristics of economical group of (RPC). The major variables in the work were steel fibers content and cement content in (RPC) case as together as exalted heating time and temperature. Tensile strength (fsp) and Compressive strength (f'c) of Reactive Powder Concrete were reach after risk to the great temperatures. Empirical results showed that the continuing strength of the Reactive Powder Concrete reduction as the risk temperature raise. More that the continuing concrete strength decreased by rising heating time. The (Vf) enhanced the mechanical characteristics of Reactive Powder Concrete at the room heat up to (150°C). Rising a temperature, decreased the continuing strength. Rising the cement contented raise the first strength of Reactive Powder Concrete, but decreasing the residuary strength values after the heating as temperature and the heating times increased.

2. Geometry of Tested RPC Deep Beams

Eleven simply supported RPC deep beams with total span (L) of 1250 mm, overall depth (h) 400mm, width 150 mm, with clear span 1050 mm. RPC deep beams are divided

into four groups ,group one represents by different volume fraction of fibers (Vf) , group two represents by different percentage of silica fume (SF), group three represents by different longitudinal reinforcement ratio (ρw) and group four represents by different the shear span to depth ratio (a/d). Table (1) illustrates all deep beams details.

Table (1) Deep Beam Details and Concrete Properties

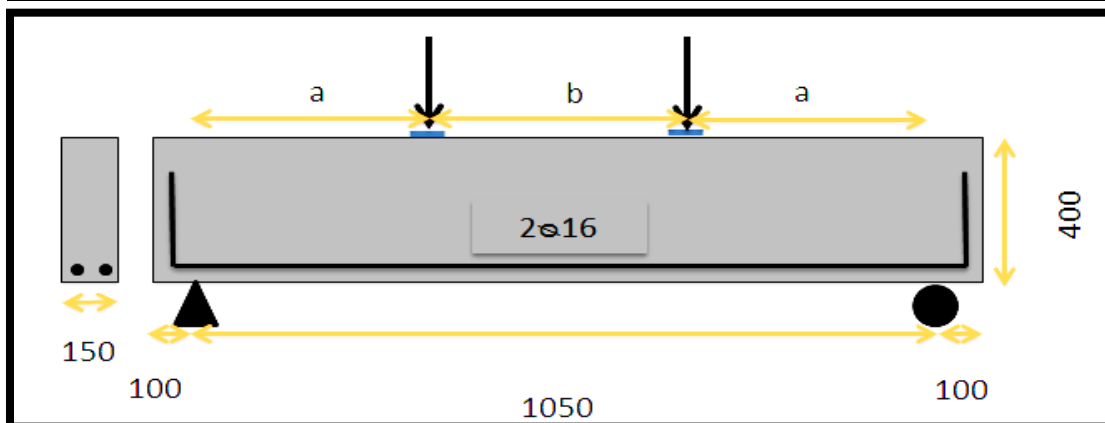| Group No.	Deep Beams	Vf %	SF %	a (mm)	b (mm)	a/d	Longitudinal Reinf.(mm)
1 (Control)	B1	0.0	15	350	350	1	2 Ø16
2 (Changing Vf)	B2	1	15	350	350	1	2 Ø16
	B3	1.5	15	350	350	1	2 Ø16
	B4	2	15	350	350	1	2 Ø16
3 (Changing SF)	B5	2	5	350	350	1	2 Ø16
	B6	2	10	350	350	1	2 Ø16
	B7	2	20	350	350	1	2 Ø16
4 (Changing ρw)	B8	2	15	350	350	1	2 Ø16+1 Ø12
	B9	2	15	350	350	1	3 Ø16
5 (Changing a/d)	B10	2	15	420	210	1.2	2 Ø16
	B11	2	15	280	490	0.8	2 Ø16

Fig.(1) Details of Typical tested Deep Beam Designed

3. Finite Element Modeling

3.1 Elements Type

Three elements is use; these elements are solid 65, link 180 and solid 185, for inspect concrete, (longitudinal steel reinforcement) and steel plates as load and supported points, respectively.

3.2 Real Constant

In the analysis, real constant set 1 used for solid 65 element, which required real constants for smeared reinforcement in the three directions x, y and z, whereas the reinforcement omitted. Therefore, this set of constants, set to zero to turn off smeared representation for reinforcement. For Solid 185, there were no real constants. Real constant set 2 was referred to link 180. This element was used to represent the longitudinal reinforcement and stirrups, the real constants of this element required information for their cross sectional area.

3.3 Material Properties

This every element, there are material piece behavior (materially characteristics). Materially piece behavior number 1 use for longitudinal reinforce (Link 180). This element demnd direct isotropic and bilinear isotropic properties as shown in Table (2). Materially model number 2 this for Solid 65, which is use for explain concrete element. This element demand direct isotropic, multi-direct isotropic and concrete parameters. Material properties for RPC used in the analysis shown in Table (3). Materially model number 3 this for steel plate (Solid 185) this loading and supporting points for averted stress concentration and crushing concrete. This inside data are this modulus of elasticity and Poisson's rate as shown in Table (4).

Table (2) Material Model Behavior for Steel Reinforcement

Material Properties for Element Link 180		
Linear Isotropic		
Modulus of elasticity, MPa	Ex	200000
Poisson's ratio	PRXY	0.3
Bilinear Isotropic		
Yield stress, MPa	Yield Stress	710 (for ϕ 12 mm) 691 (for ϕ 16 mm)
Tangent Modulus, MPa	Tang Mod	6000

Table (3) Material Model Behavior for Concrete

Material Properties for Element Solid 65		
Linear Isotopic		
Modulus of elasticity, MPa	Ex	44240
Poisson's ratio	PRXY	0.2
Multi Linear Isotropic		
Points Number	Strain	Stress, MPa
1	0.000774	29
2	0.001548	53
3	0.002322	70
4	0.003097	81
5	0.003871	87
6	0.004645	92

| Concrete Parameters		
Shear transfer coefficients for an open crack	ShrCf-Op	0.18
Shear transfer coefficients for a close crack	ShrCf-Cl	0.2
Uniaxial tensile cracking stress, MPa.	UnTensSt	14.3 *
Uniaxial crushing stress (positive), MPa.	UnCompSt	92 **

*Depends on the tensile strength of deep beams

** Depends on the compressive strength of deep beams

Table (4) Material Model Behavior for Steel Plates

Material Properties for Element Solid 185		
Linear Isotopic		
Modulus of elasticity, MPa	Ex	200000
Poisson's ratio	PRXY	0.3

3.4 Geometry

This finite element analysis, tested deep beams experimentally, modeled with take advantaging from this symmetry of the deep beams supports and loadings. The finite element mesh for quarter of this deep beam as shown in Figure (2).
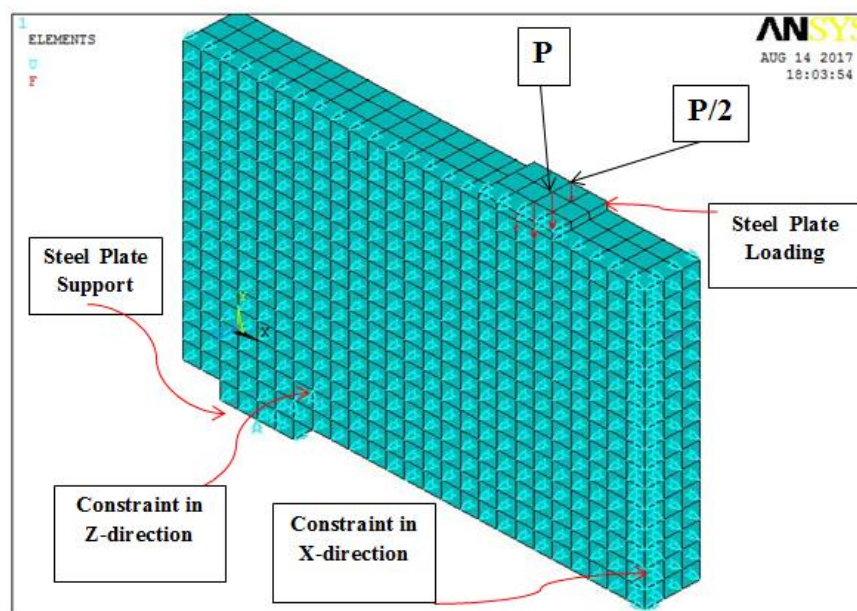
Figure(2) Geometry of the Ansys Model for Deep Beam

Discrete representation (Link 180) is use for mode all types of reinforcement (longitudinal reinforcement). With the advantaging from discrete model, the longitudinal reinforcement in tension were protected in their real position. Details from reinforced between concrete elements are shown in Figure (3).
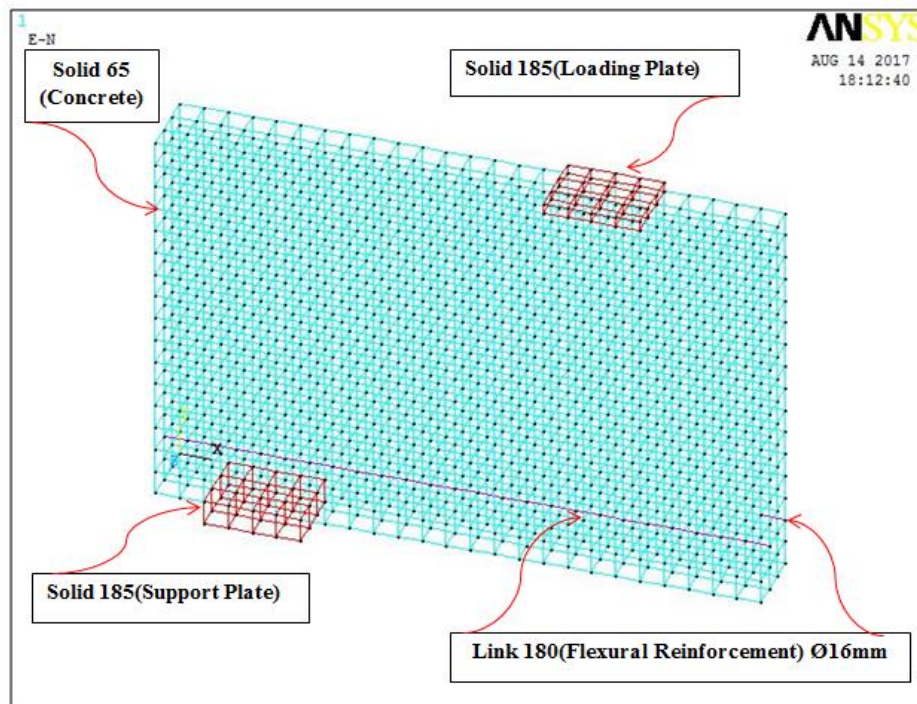
Figure (3)Details of Reinforcement

3.5 Loads and Boundary Conditions

In the experimental work, concentrated load were applied at the mid-point of each span over a bearing plate with dimensions (150) mm length, (100) mm width and (10) mm thickness. The applied load was represented by dividing the total distributed load on the top nodes according to the area surrounded by each node to represent the distributed load in ANSYS program as shown in Figure (4). The supports were approximately as similar as in the experimental work.
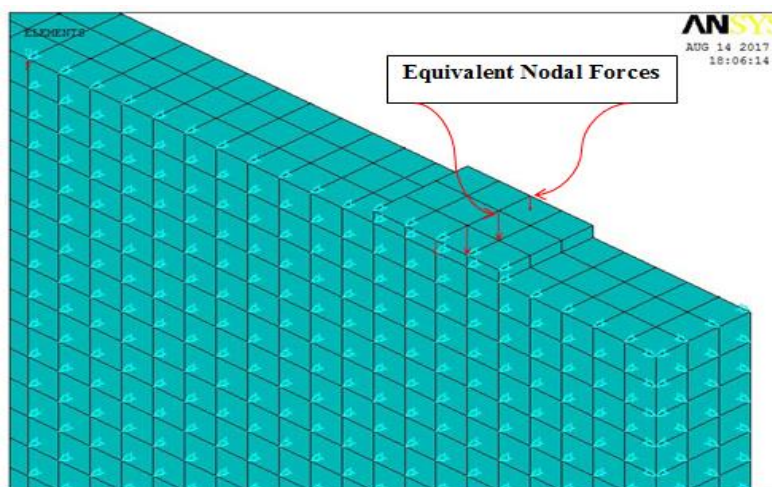

Figure (4) Details of Applied Load Boundary Conditions

4. Results of Finite Element Analysis

The results of finite element analysis using ANSYS program were compared with the experimental results for all tested deep beams. The numerical failure was similar to the failure mode of each deep beam that occurred in experimental work. ANSYS results including ultimate load, load-deflection response and crack patterns where a close to the experimental results.

4.1 Cracking Loads

Table (5) shows the comparison between the cracking loads of the experimental (tested) deep beams, $P_{cr)exp.}$, and the theoretical cracking loads from the finite element models, $P_{cr)theo.}$. A good agreement is shown between the cracking loads of the experimental deep beams and the theoretical cracking loads from the finite element models as shown in the table below.

Table (5) Comparison between experimental and theoretical cracking loads

Specimen	Cracking Load (kN)		$\dfrac{P_{cr)theo.}}{P_{cr)exp.}}$
	$P_{cr)exp.}$	$P_{cr)theo.}$	
B1	75	80	1.06
B2	120	121	1.01
B3	120	121	1.01
B4	140	145	1.04
B5	100	102	1.02
B6	125	126	1.01
B7	175	178	1.01
B8	150	152	1.01
B9	220	223	1.01
B10	90	92	1.02
B11	150	154	1.03

### 4.2 Numerical Ultimate Load

The comparison between the ultimate load from the experimental results and numerical models from finite element analysis of the analyzed deep beams are listed in Table (6). The difference between the experimental ultimate load and that obtained by finite element analysis is not more than (4.2) %.

Table (6) Experimental and Numerical Ultimate Loads for all Tested deep Beams

| Specimens	Ultimate Load(KN)		Fu) Theo/ Fu)EXP. (%)
	Fu)EXP.	Fu)ANSYS	
B1	840	849	1.011
B2	310	323	1.042
B3	720	732	1.016
B4	805	812	1.009
B5	680	700	1.029
B6	760	774	1.018
B7	1090	1097	1.006
B8	1025	1039	1.014
B9	1250	1254	1.003
B10	730	754	1.033
B11	1040	1040	1.000

4.3 Load-Deflection Curves

The load-deflection curve for each deep beam obtained from the finite element analysis together with the experimental curves are presented and compared in figures from (5) to (15). In general, all these figures show a good agreement between this experimental and F.E.A curves.
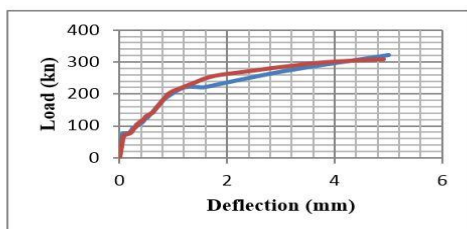
Fig(5)–B1
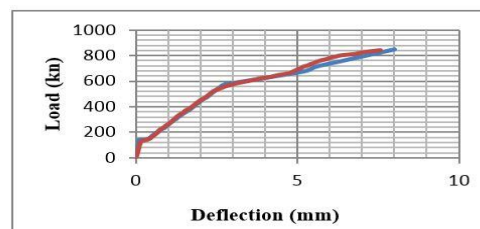
Fig(8)–B4

Fig(6)–B2

Fig(9)–B5

Fig(7)-B3

Fig(10)-B6
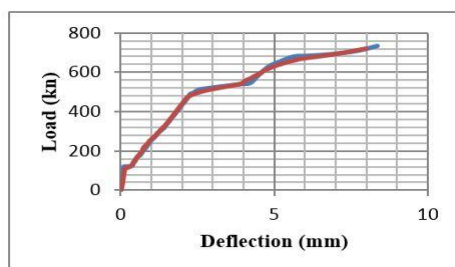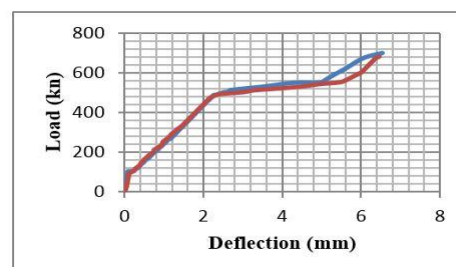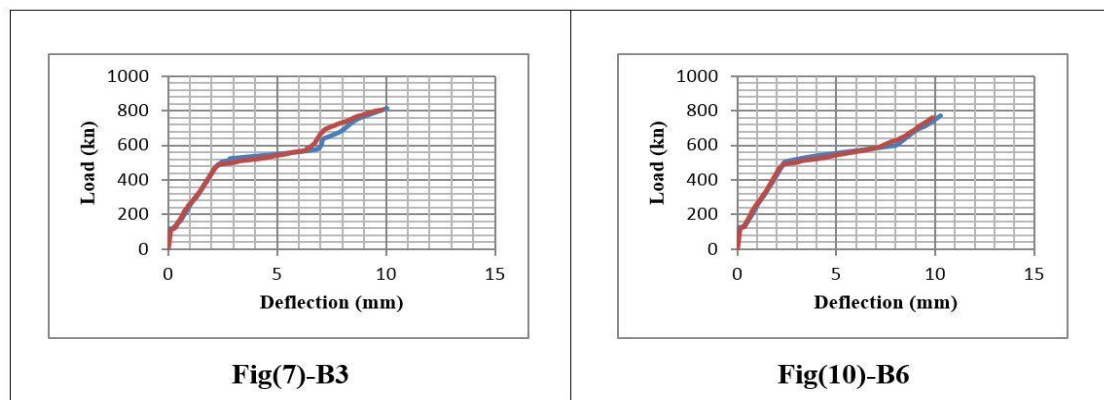
Figures from (5) to (10) Compared Experimental (____) and ANSYS (____) Load Deflection Curve for Deep Beam

Fig(11)-B7

Fig(13)-B9

Fig(12)-B8

Fig(14)-B10

Fig(15)-B10
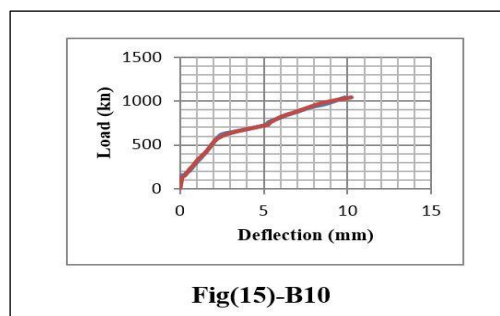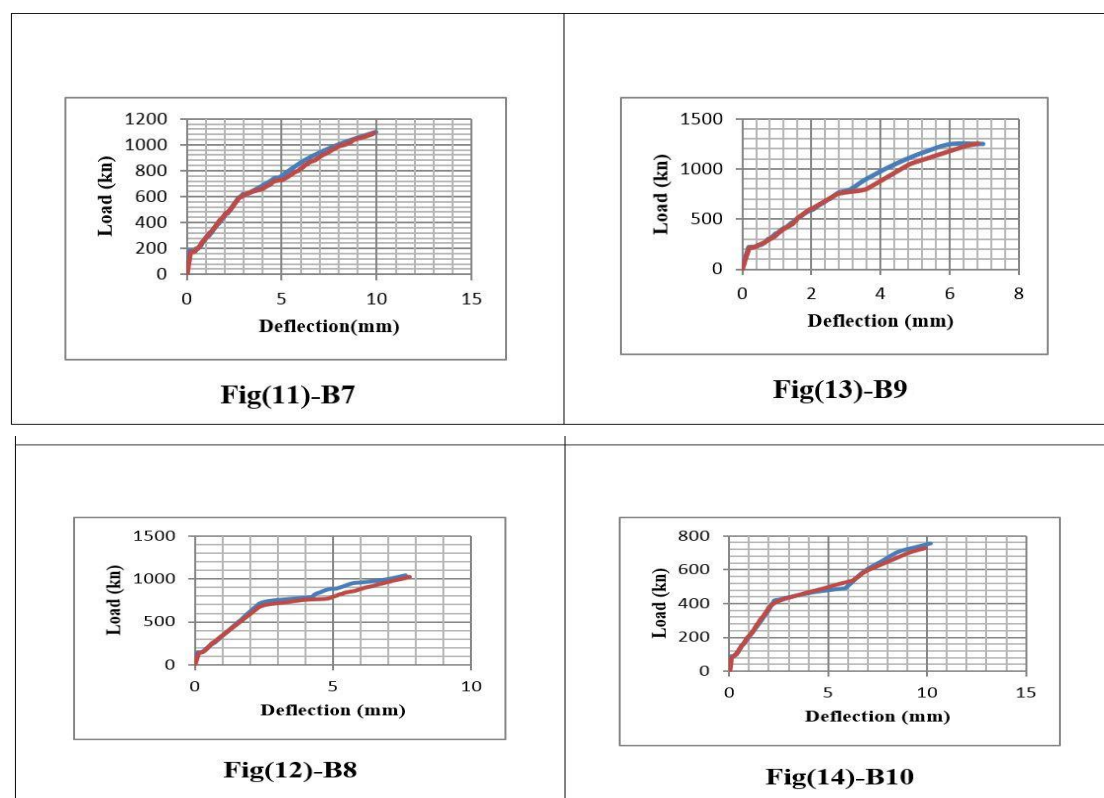
Figures from (11) to (15) Compared Experimental (____) and ANSYS (____) Load Deflection Curve for Deep Beam

4.4 Crack Patterns

The numerical-model painted the cracks at all stages of loading. Cracking-patterns in the deep beams was obtained using the Crack Crushing plot option in ANSYS (V.11). According to ANSYS program, the first crack which represented slight crack is symbolized by a red circle outline at an integration point, the second crack which represents moderate crack is symbolized by a green circle outline, and the third crack which represents failure crack is symbolized by a blue circle outline. The results showed a good agreement in crack patterns and failure mode between numerical and experimental tested deep beams as shown in Fig. (16) and Fig. (17).
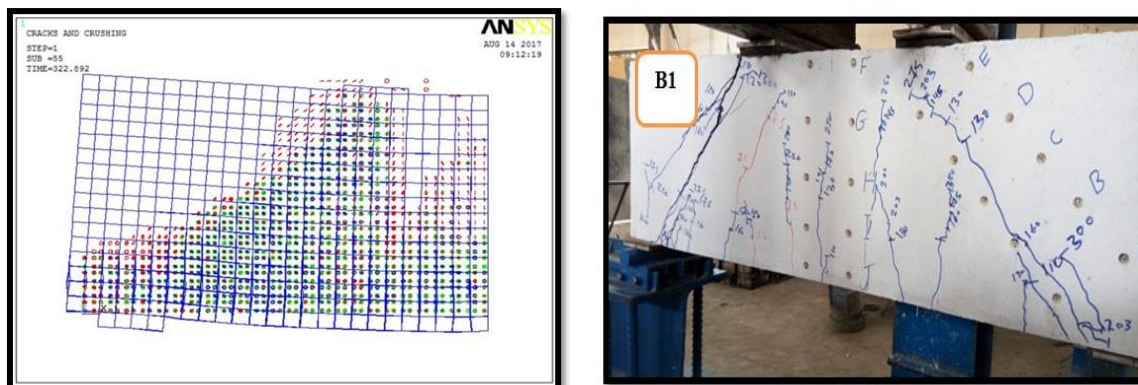

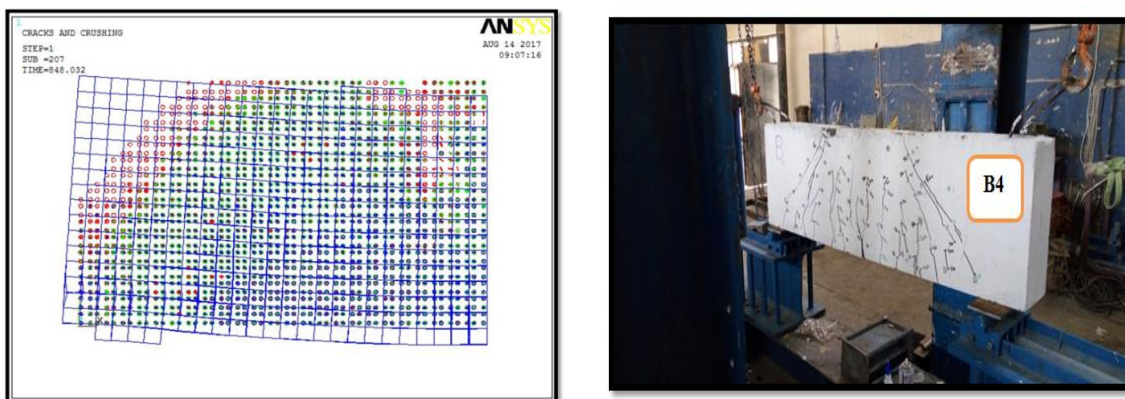**Fig (16) Crack Pattern for Deep Beam Control (B1) at Failure Load, without (Vf)**

Fig (17) Crack Pattern for Deep Beam (B4) at Failure Load, content (Vf)

4.4.1 Deep Beams Failing in Diagonal Tension

The stages in the crack pattern development for a deep beam failing eventually in diagonal tension are as follows:

1. At low loads, short vertical flexural cracks were observed in the region of pure bending, between the two point load positions of the deep beam.

2. With further increase in load, additional flexural cracks are formed vertically in the central region and new flexural cracks are formed in the shear spans between point load

and support. These latter cracks gradually became inclined as they propagated to regions above the longitudinal reinforcement and curved toward the loading point.

3. With further increase in load, diagonal inclined cracks were generally initiated in the shear span at a position approximately mid-depth of the RPC deep beam. In most of the tested deep beams these diagonal cracks were formed in both shear spans at the same load level or little different.

4. Cracks propagation continued, the flexural cracks in the central region extended vertically, the inclined cracks which were formed from the initiating flexural cracks extended toward the point load. The diagonal cracks initiating in the shear span extended toward the point load in the one direction and nearly horizontally at the level of the longitudinal reinforcement towards the support in the other direction. In some deep beams these diagonal cracks met the flexural cracks or the inclined cracks formed from the initiating flexural cracks.

5. Finally, one of the diagonal cracks extended in the compressive zone towards the point load causing failure. This failure behavior can be considered as a mode of diagonal tension failure.

4.4.2 Deep Beams Failing in Shear-Flexure

The crack pattern development for a shear-flexure failure is the same as that described for a diagonal tension failure up to stage 4. At stage 5, the width of the diagonal crack increased gradually with increasing load and finally, the crushing occurs suddenly on the top surface of the deep beam and extends downwards through the compression zone, causing failure in the region of pure bending, between the two point loads of the deep beam.

5. Test Results

5.1 Effect of Volume Fraction of Steel Fibers (Vf)

To show the role of the presence of the steel fibers on the load- mid span deflection curves of RPC deep beams, the load-deflection curves for each otherwise identical four deep beams B1, B2, B3 and B4 with 0.0, 1.0, 1.5 and 2 % volume fraction of steel fibers respectively. Each one of these curves initiates in a linear form with a constant slope, changes to a nonlinear form with varying slope. Then, the third stage starts when the deflection increases rapidly with small increase in the load. It is clear from the figure that at early stages of loading, the deflection decreases as the volume fraction of fibers is increased. This behavior may be attributed to enhanced stiffness of RPC deep beams and improving the mechanical properties of RPC concrete such as (modulus of elasticity, tensile strength and compressive strength) when the amount of steel fibers is increased. The additions of steel fibers to RPC deep beams at volume fractions of 1.0 % in B2, 1.5% in B3and 2 % in B4 results in an increase of in the deflection at ultimate load, respectively compared with non-fibrous RPC deep beam B1 (Vf=0.0). This is normally explained by the efficiency of steel fibers in arresting the propagation and controlling the growth of the flexure and diagonal cracks within the deep beam when they are crossed by them, and hence, steel fibers maintain the deep beam integrity throughout the post

cracking stages of behavior. The deep beam, hence could withstand greater loads and deflection before failure.

5.2 Effect of Adding Different Percentages of (SF) Powder

The effect of three percentages of silica fume SF on the load-deflection behavior. It is clear from this figure that for the same load level, the deflection decreases with the increase in SF content. This is related to enhanced particle packing density and intensive chemical reaction due to pozzolanic reaction with silica hydrate conversion which led to increasing bond between RPC matrix and steel fibers. Therefore any increase in SF content enhances the crack control and decreases the deflection of the RPC deep beam at the same load level. Thus, increasing SF from 5% in B5, 10% in B6 and 20% in B7 results in a decrease in their deflections at ultimate load of 14% , 31% and 30.5% compared with those of deep beam control B4 (SF =15%), respectively.

5.3 Effect of Longitudinal Reinforcement Ratio (ρw)

As would be expected, at a same load level, the deflection decreases with the increase of (ρw). This is due to the fact that any increase in (ρw) enhances the crack control and prevents the flexural cracks from further widening and hence decreases the deflection of the RPC deep beam at the same load level. By comparing the load-deflection response of deep beams B4 (ρw =0.00765), B8 (ρw =0.00981) and B9 (ρw =0.01148), a steady decrease in deflection with rising (ρw) values is indicated. It can be shown that the deflection at ultimate load dropped by 2.6% and 9.9% respectively for B8 and B9, when compared with B4. This was actually expected and is almost related to the considerable decrease in the tensile strain of the reinforcing bars which act as a tension chord for the remaining tied arch after the propagation of the diagonal crack and flexure crack. Since this tensile strain of the reinforcing bars contributes much to the opening up of the diagonal and flexure cracks, it causes a decrease in deflection at ultimate load when increasing (ρw).

5.4 Effect of Shear Span to Effective Depth Ratio (a/d)

The load-deflection curves for RPC deep beams, a given load level at early stages of loading, the deflection increases with increasing shear span to effective depth ratio (a/d). Also, the deflection at ultimate load decreases with the increase in (a/d). As shown by the results of RPC deep beams when Vf =2%, the increase in (a/d) ratio from 1 to 1.2 causes the increase (31%) in their deflections at ultimate load, respectively compared with RPC deep beam B4 (a /d =1), while the decrease in (a/d) ratio form 1 to 0.8 causes an decrease (35 %) in their deflections at ultimate load, respectively compared with RPC deep beams B4 (a /d =1).

6. Conclusions

1. The non-linear finite element analysis by using ANSYS program of RPC deep beams this the powerful technique and the can supply this researchers with valuable information. They are three-dimensional FEM adopting in this present work, is suitable to predict the behaviour of RPC deep beams failing in shear. The numerical results were in good agreement with the experimental load-deflection curves of the tested RPC deep beams throughout the entire range of behavior.

2. This compare between the numerical and experimental results asserted the validity of the numerical analysis and the methodology developed where the maximum difference ratio in ultimate load was less than 4.2 % for all the tested and analyzed RPC deep beams.

3. The amount of steel fibers in RPC mixture has significantly affect the initial diagonal cracking load and influences the ultimate load. By increasing the volume fraction of fibers from 0% to 1.0%, 1.5%, and 2.0%, the diagonal cracking load increases by 46.7%, 60.0% and 86.7% as compared with nonfibrous RPC deep beam, respectively. Also for the same increase in the volume fraction of fibers the ultimate failure increases by 132%, 159.6% and 171% as compared with the nonfibrous RPC deep beam, respectively.

4. The amount of steel fibers in RPC mixture has significantly effect on the ultimate crack width. By increase in the volume fraction of fibers the ultimate crack width decreases by 82.5%, 90% and 92.5% as compared with the nonfibrous RPC deep beam, respectively.

5. The amount of silica fume on the RPC mixture has significantly affect the initial diagonal cracking load and influences the ultimate load. By increasing the percentage of silica fume from 5% to 10%,15% and 20%, the diagonal cracking load increases by 25.0%, 40.0% and 75.0% , respectively. Also for the same percentage increase in the silica fume the ultimate failure increases by 11.8%, 23.5% and 60.3% as compared with the B5 RPC deep beam, respectively.

6. The amount of silica fume in RPC mixture has significantly effect on the ultimate crack width. By increase in the silica fume the ultimate crack width decreases by 41.7%, 78.3% and 85.0% as compared with the B5 RPC deep beam, respectively.

7. The amount of steel reinforcement in RPC mixture has significantly affect the initial diagonal cracking load and influences the ultimate load. By increasing the steel reinforcement from 0.765% to 0.981% and 1.148%, the diagonal cracking load increases by 7.0% and 57.0% as compared with B4 RPC deep beam, respectively. Also for the same increase in the steel reinforcement the ultimate failure increases by 22% and 48.8% as compared with B4 RPC deep beam, respectively.

8. The amount of steel reinforcement in RPC mixture has significantly effect on the ultimate crack width. By increase in the steel reinforcement the ultimate crack width decreases by 44% and 52% as compared with the B4 RPC deep beam, respectively.

9. The changing in (a/d) ratios has significantly effect on the initial diagonal cracking load and the ultimate load. By increasing the (a/d) ratio from 1 to 1.2, the diagonal cracking load and the ultimate load decreases by 35.7% and 13%, respectively. Furthermore the changing in (a/d) ratios has significantly effect on the ultimate crack width and the deflection of ultimate load. By increasing the (a/d) ratio from 1 to 1.2, the ultimate crack width and the ultimate deflection increases by 185.7% and 83.6%, respectively.

10. The changing in (a/d) ratios has significantly effect on the initial diagonal cracking load and the ultimate load. By decreasing the (a/d) ratio from 1 to 0.8, the diagonal

cracking load and the ultimate load increase by 7% and 23.8%, respectively. Furthermore the changing in (a/d) ratios has significantly effect on the ultimate crack width and the deflection of ultimate load. By decreasing the (a/d) ratio from 1 to 0.8, the ultimate crack width and the ultimate deflection decrease by 28% and 16.5%, respectively.

References

[1] Sadrekarimi, A., "Development of a Light Reactive Powder Concrete", Journal of Advanced Concrete Technology Vol. 2, No. 3, Japan Concrete Institute., pp. 409-417, 2004.

[2] ACI Committee, " Building Code Requirements for Structural Concrete (ACI 318-14) and Commentary (ACI 318R-14), American Concrete Institute", Farmington Hills, MI, 519 pp, 2014.

[3] ANSYS Help,"ANSYS User's Manual", SAS IP, Inc., Version 11.0, U.S.A. Cook, R.D. 1974, "Concept and Application of Finite Element Analysis", John Wilely and Sons, Inc., New York, 2011.

[4] Kadri , E. H., Aggoun ,S., S. Kenai and Kaci, A., "The Compressive Strength of High-Performance Concrete and Ultrahigh-Performance", Hindawi Publishing Corporation, Advances in Materials Science and Engineering,7 p, 2012.

[5] Bashandy, A. A., "Influence of Elevated Temperatures on the Behavior of Economical Reactive Powder Concrete", Journal of Civil Engineering Research, 3(3): 89-97 DOI: 10.5923/j.jce.20130303.01, 2013.

[6] Voo, J. Y. L., Foster, S. J., Gilbert, R. I. and Gowripalan, N., "Behavior of Reactive Powder Concrete Deep Beams", Advances in Mechanics of Structures and Materials, N., PP.235-240, 2002.

[7] Gao, R., Stroeven, P., and Hendriks, C. F., "Mechanical Properties of Reactive Powder Concrete Beams", ACI Special Publications, Vol.2, No.228, PP.1237-1252, 2005.

[8] Graybeal, B. A., and Hartmann, J. "Strength and Durability of Ultra-High Performance Concrete." Proc., Concrete Bridge Conference.

[9] Ali, H. A., "Structural Behavior of Reactive Powder Concrete Member under Repeated loads" PhD thesis University of Babylon, 2015.

رغيد فتحي مكي

قسم الهندسة المدنية، جامعة الكوفة، الكوفة، العراق

Ragheed.Almutwali@uokufa.edu.iq

علي طالب جاسم

قسم الهندسة المدنية، جامعة الكوفة، الكوفة، العراق

alit.albozwaida@uokufa.edu.iq

أصيل سلطان رضا

قسم الهندسة المدنية، جامعة الكوفة، الكوفة، العراق

aseel.aseel.1979@gmail.com

الخلاصة

في هذا العمل، تم اجراء تحليل لا خطيا بالعناصر المحددة باستخدام برنامج ANSYS V.11 لأحدى عشر من الأعتاب العميقة من خرسانة المساحيق الفعالة المفحوصة مختبريا، لها أبعاد 150 ملم عرض، 400 ملم عمق و1250 ملم الطول العتب. الهدف من البحث هو استعمال التحليل اللاخطي بواسطة العناصر المحددة (Finite Elements) ثلاثية الأبعاد كوسيلة عددية لدراسة وتحري تصرف هذه العتبات الخرسانية العميقة للمساحيق الفعالة باستخدام البرنامج (ANSYS V.11) حيث تم في هذا البرنامج تمثيل الجزء الخرساني باستخدام العناصر الطابوقية ذات الثمانية عقد (Solid 65) وتم استخدام عنصر ثلاثي الابعاد (LINK180) لتمثيل حديد التسليح وتم استخدام عنصر ثلاثي الابعاد (LINK185) لتمثيل صفيحة (بليت) حديد. تمت المقارنة ما بين النتائج العملية المستحصلة من الفحوصات المختبرية السابقة مع تلك النتائج النظرية المستحصلة من التحليل اللاخطي بواسطة العناصر المحددة ثلاثية الابعاد حيث اظهرت النتائج النظرية توافقا" جيدا" مع تلك النتائج العملية، حيث كانت أكبر نسبة مئوية للفرق في التحميل الأقصى للانحناء اقل من (4.2%).

الكلمات المفتاحية: التحليل اللاخطي، العناصر المحددة ثلاثية الأبعاد، خرسانية المساحيق الفعالة، الأعتاب العميقة.